Topology-like dynamical behavior of magnetization reversal in exchange-bias systems*

Su Yuan-Chang(苏垣昌)[a], Zhang Li-Juan(张丽娟)[a], Yang Xin(杨 鑫)[b], Pan Jing(潘 靖)[a], and Hu Jing-Guo(胡经国)[a]†

[a] College of Physics Science and Technology, Yangzhou University, Yangzhou 225002, China
[b] School of Physics and Technology, Nanjing Normal University, Nanjing 210023, China

(Received 20 November 2012; revised manuscript received 31 December 2012)

In an exchange-bias system, the barriers with intrinsic potential energy may be asymmetric due to unidirectional anisotropy. Based on the Stoner–Wohlfarth model, we show that the asymmetric barriers may lead to four kinds of dynamical process underlying the hysteresis-loop measurement. These kinds of dynamical processes are different in a topology-like property, which can be controlled by the orientation of the external field. In our study, a new analysis approach has been proposed to reveal the dynamical behaviors of magnetization reversal. With this approach, coercivity, exchange-bias field, and asymmetry of hysteresis loops can be quantitatively obtained.

Keywords: exchange-bias system, intrinsic energy potential, magnetization reversal

PACS: 75.70.Cn, 75.30.Gw, 75.30.Et **DOI:** 10.1088/1674-1056/22/7/077503

1. Introduction

In ferromagnet (FM)/antiferromagnet (AFM) bilayer systems, interface exchange coupling may induce a unidirectional anisotropy when the FM/AFM system is cooled below the Néél temperature of the AFM in a static external magnetic field.[1–8] The unidirectional anisotropy leads to the phenomenon of exchange bias (EB),[1,9] and plays a crucial role in magnetization reversal.[10–13] In such EB systems, the unidirectional and uniaxial anisotropies may be noncollinear and the hysteresis loop may exhibit asymmetric magnetization reversal (AMR).[14–26] In the past decade, noncollinear anisotropies and AMR have been extensively studied. It was suggested that the AMR originates from different magnetization reversal mechanisms for the descent and ascent branch of a hysteresis loop.[13,20] For example, the coherent rotation of the magnetization is the main mechanism for the ascent branch, whereas the mechanism for the descent branch changes to the domain wall nucleation and propagation.[13] However, there are still ongoing controversies on the basic mechanism of AMR.[16]

In this paper, the effect of the unidirectional anisotropy on the intrinsic potential energy (IPE) and the effect of the IPE on the dynamical behavior of magnetization reversal (DBMR) are investigated using the Stoner–Wohlfarth model.[27] Firstly, we show that a novel effective easy axis, which is no longer a line, may emerge due to the competition between the uniaxial anisotropy and the unidirectional anisotropy. The noncollinearity between the unidirectional anisotropy and the uniaxial anisotropy can be detected by the angle between the two easy orientations of magnetization. Secondly, we show that the distribution of the stable equilibrium states of magnetization plays a crucial role in understanding the DBMR. There are two basic mechanisms of magnetization reorientation in hysteresis-loop measurement (HLM), namely continuous-rotation and abrupt-flop. The continuous-rotation happens when there are continuous stable equilibrium states, whereas the abrupt-flop happens when there is no stable equilibrium state. All together, we find four kinds of dynamical processes underlying the hysteresis-loop measurement, which can be distinguished by a topology-like property. Different kinds of dynamical processes exhibit different histories in magnetization transversal across the barriers of IPE.

2. Model and method

An EB system can be treated as an FM monolayer with an additional unidirectional anisotropy.[12] Based on the Heisenberg lattice model, the Hamiltonian can be written as

$$H = -J\sum_{\langle i,j\rangle}\boldsymbol{S}_i\cdot\boldsymbol{S}_j-\sum_i D^x(S_i^x)^2 -\sum_i \boldsymbol{K}\cdot\boldsymbol{S}_i-g\mu_{\rm B}\sum_i \boldsymbol{h}\cdot\boldsymbol{S}_i, \quad (1)$$

where J is the exchange-coupling constant which is nonzero only for nearest-neighbor spins, D^x is the uniaxial anisotropic constant, and K denotes the unidirectional anisotropy. The fourth term is the Zemman energy, and g, $\mu_{\rm B}$, and h represent the Lande factor, the Bohr magneton, and the external field, respectively. The effective field acting on each spin $\boldsymbol{S}_i$ can be obtained by $\boldsymbol{h}^i_{\rm eff}=-\partial H/(\partial\boldsymbol{S}_i)$. Explicitly, we have

$$\boldsymbol{h}^i_{\rm eff}=\sum_{j(\neq i)} J\boldsymbol{S}_j+2D^xS_i^x\boldsymbol{e}_x+\boldsymbol{K}+g\mu_{\rm B}\boldsymbol{h}. \quad (2)$$

*Project supported by the National Natural Science Foundation of China (Grant Nos. 10974170 and 11104239) and the Natural Science Foundation of Jiangsu Province, China (Grant No. 09KJB140011).

†Corresponding author. E-mail: jghu@yzu.edu.cn

© 2013 Chinese Physical Society and IOP Publishing Ltd

The IPE that includes the energies of exchange interaction and anisotropies can be defined as

$$E_{\rm p} = -\sum_i \boldsymbol{S}_i \cdot \boldsymbol{h}^i_{\rm In},$$
$$\boldsymbol{h}^i_{\rm In} = \sum_{j(\neq i)} J\boldsymbol{S}_j + 2D^x S^x_i \boldsymbol{e}_x + \boldsymbol{K}, \quad (3)$$

where $\boldsymbol{h}^i_{\rm In}$ is the intrinsic effective field acting on $\boldsymbol{S}_i$. In the Stoner–Wohlfarth model, the total spin is $\boldsymbol{S} = N\boldsymbol{S}_i$, where N is the number of spins. The equilibrium state of the system can be determined by the criterion that $\boldsymbol{S}$ is parallel to the effective field $\boldsymbol{h}_{\rm eff}$. Based on this criterion, the magnitude of external field in any equilibrium states denoted by $(\varphi_{\rm S}, \varphi_{\rm K}, \varphi_{\rm h})$ can be given by

$$h = \frac{2D\sin\varphi_{\rm S}\cos\varphi_{\rm S} + K(\cos\varphi_{\rm K}\sin\varphi_{\rm S} - \sin\varphi_{\rm K}\cos\varphi_{\rm S})}{\sin\varphi_{\rm h}\cos\varphi_{\rm S} - \cos\varphi_{\rm h}\sin\varphi_{\rm S}}, \quad (4)$$

where $\varphi_{\rm S}$, $\varphi_{\rm K}$, and $\varphi_{\rm h}$ are the angles between $\boldsymbol{S}$, $\boldsymbol{K}$, $\boldsymbol{h}$ and the x axis (the easy axis), respectively. For simplicity, the magnitude of each spin has been set as $|\boldsymbol{S}_i| = 1$. From Eq. (4), any equilibrium state under a given external field $\boldsymbol{h}$ can be obtained. It should be noted that the equilibrium states obtained from Eq. (4) may be stable or unstable. Generally, only some of the stable equilibrium states emerge in a particular magnetization process. A set of stable equilibrium states in the HLM may reveal the DBMR.

3. Intrinsic potential energy

Figure 1 shows $E_{\rm p}$ as a function of $\varphi_{\rm S}$ under different K and $\varphi_{\rm K}$. The uniaxial anisotropic constant is $D^x = 0.1J$. When K is small, there are two maxima and two minima in the curves of IPE. When K increases, the positions of maxima and minima may change gradually. In the utmost limit, only one maximum and one minimum remain in the curves of IPE, and their positions can be obtained by $\varphi_{\rm S} = 2\pi - \varphi_{\rm K}$ and $\varphi_{\rm S} = \varphi_{\rm K}$, respectively. Figure 1(a) shows the case of collinear anisotropies. In this case, the curves of IPE is symmetric. As K increases, two maxima move together gradually while two minima keep still. When there is an angle between the uniaxial anisotropy and the unidirectional anisotropy (see Figs. 1(b) and 1(c)), the curves of IPE are asymmetric. In these cases, both two maxima and two minima move together gradually as K increases. Figure 1(d) shows the case in which the unidirectional anisotropy is perpendicular to the uniaxial anisotropy. In this case, two maxima keep still and two minima move together gradually as K increases. The change in the positions of maxima and minima indicates the variation of the hard and easy orientations of magnetization, respectively.

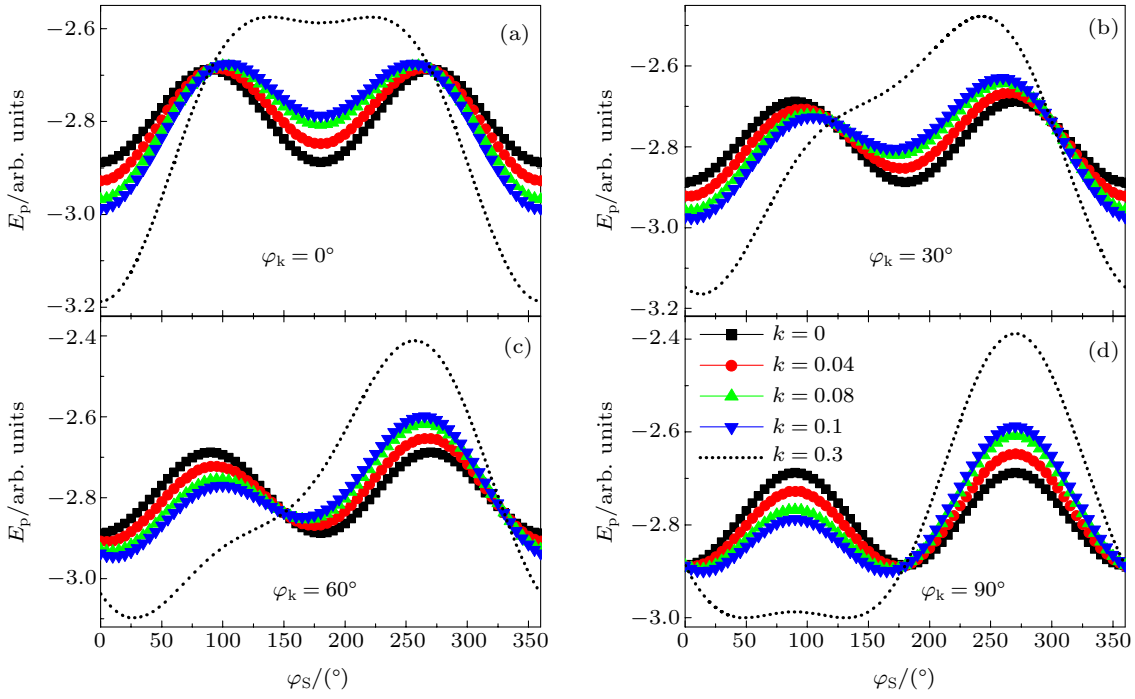


Fig. 1. (color online) Dependence of $E_{\rm p}$ on $\varphi_{\rm S}$ under different K and $\varphi_{\rm K}$. (a) $\varphi_{\rm K} = 0°$; (b) $\varphi_{\rm K} = 30°$; (c) $\varphi_{\rm K} = 60°$; (d) $\varphi_{\rm K} = 90°$.

Generally, there are two maxima and two minima in the IPE curve, as shown in Fig. 2(a). These two minima, marked by φ_1 and φ_2, denote two easy orientations of magnetization of the system. If there is no unidirectional anisotropy, namely in an FM just with a uniaxial anisotropy, we have $\varphi_1 = 0°$ and $\varphi_2 = 180°$. However, figure 2(a) shows that $\Delta\varphi_1 = \varphi_1 - 0°$ and $\Delta\varphi_2 = 180° - \varphi_2$ can be nonzero in an EB system. The angle between the two easy orientations of magnetization, $\Delta\theta = \varphi_2 - \varphi_1$, is less than 180°. These results indicate that the effective easy axis deviates from the uniaxial anisotropic axis (easy axis), and is not a line any more, as shown in Fig. 2(b). The noncollinearity between the unidirectional anisotropy and

the uniaxial anisotropy can be judged by $\Delta\theta < 180°$.

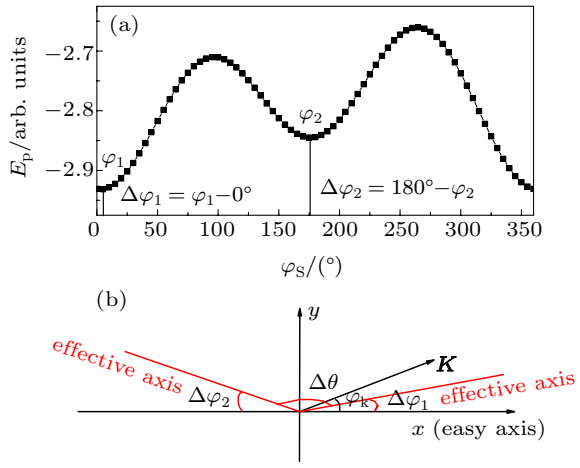


Fig. 2. (color online) Schematic of the effective easy axis. (a) Typical E_p as a function of φ_S under parameters $K = 0.06$ J/μ_B and $\varphi_K = 30°$. (b) The corresponding effective easy axis characterized by $\Delta\varphi_1$, $\Delta\varphi_2$, and $\Delta\theta$.

4. Dynamic behavior of magnetization reversal

In order to investigate the effect of the IPE on DBMR, we calculate the external field h as a function of φ_S by Eq. (4). Two typical cases with parameter $K = 0.06J/\mu_B$ are investigated.

Figure 3 shows h and E_p as functions of φ_S in the case of collinear anisotropies, namely $\varphi_K = 0°$. The process of HLM is shown by solid curves and dotted arrows. In the area of dotted arrows, there is no stable equilibrium state, and $\boldsymbol{S}$ undergoes an abrupt-flop process across a barrier of IPE.

Figure 3(a) shows the case of $\varphi_h = 0°$. The process $1 \to 2 \to 3 \to 4 \to 1$ forms the whole HLM, which is composed of two abrupt-flop processes, namely $2 \to 3$ and $4 \to 1$. The $\boldsymbol{S}$ may transverse one or two barriers of IPE. Obviously, H_E is nonzero and the hysteresis loop is symmetric. Figure 3(b) shows the case of $\varphi_h = 10°$. The whole HLM ($1 \to 2 \to 3 \to 4 \to 5 \to 6 \to 2 \to 1$) consists of two continuous-rotation processes and two abrupt-flop processes. The $\boldsymbol{S}$ transverses two barriers. In this case, H_E is nonzero and the hysteresis loop is asymmetric. Figure 3(c) shows the case of $\varphi_h = 90°$. The whole HLM ($1 \to 2 \to 3 \to 2 \to 1$) is completed by a reversible continuous-rotation process. The $\boldsymbol{S}$ does not transverse any barrier. The descent branch and ascent branch completely overlap. We obtain $H_d = H_a = h(\varphi_S = 0°) = 0$, so both H_C and H_E are equal to zero.

Figure 4 shows h and E_p as functions of φ_S when $\varphi_K = 30°$. In the case of noncollinear anisotropies, the HLM may exhibit new characteristics in comparison with Fig. 3. When $\varphi_h = 0°$, as shown in Fig. 4(a), the whole HLM ($1 \to 2 \to 3 \to 4 \to 5 \to 6 \to 2 \to 1$) consists of two continuous-rotation processes and two abrupt-flop processes. The $\boldsymbol{S}$ just transverses the lower barrier. The EB field H_E is nonzero and

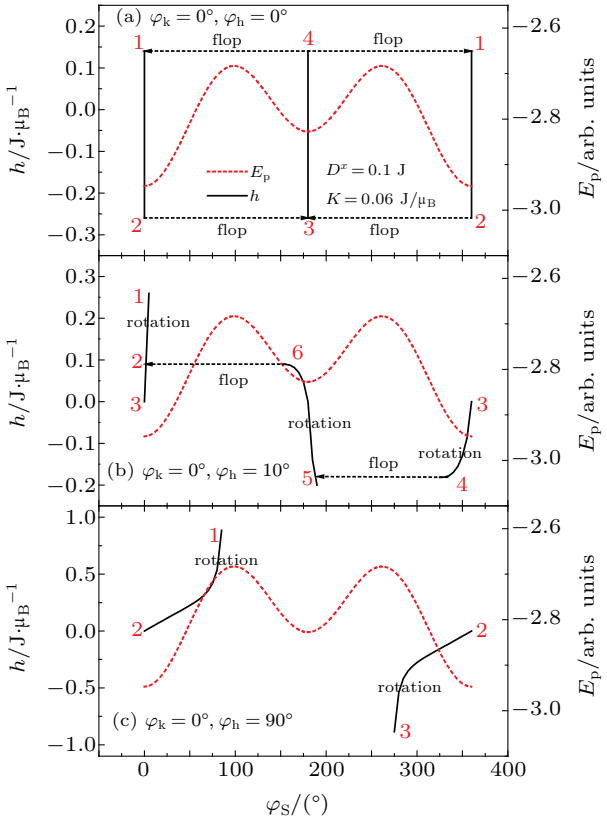


Fig. 3. (color online) Dependences of h and E_p on φ_S under different φ_h. (a) $\varphi_h = 0°$; (b) $\varphi_h = 10°$; (c) $\varphi_h = 90°$. The solid curves denote the stable equilibrium states occurring continuously in the HLM, where the spin rotates continuously. The dotted arrows denote the spin switches in the descent branch or ascent branch of the hysteresis loop.

the hysteresis loop is asymmetric. As φ_h increases, the HLMs in Fig. 4(b) ($\varphi_h = 10°$) and Fig. 4(c) ($\varphi_h = 90°$) are similar to that in Figs. 3(b) and 3(c), respectively. We divide it into three regions: i) when $0° \le \varphi_h < 7°$, the HLMs belong to the same kind as that shown in Fig. 4(a); ii) when $7° < \varphi_h < 76°$, the HLMs belong to the same kind as that shown in Fig. 4(b); iii) when $76° < \varphi_h \le 90°$, the HLMs belong to the same kind as that shown in Fig. 4(c).

According to the above analysis, there are four different kinds of dynamical processes underlying HLM, as shown in Figs. 3(a) and 4(a), Figs. 3(b) and 4(b), and Figs. 3(c) and 4(c), respectively. These kinds of dynamical processes can be distinguished by a topology-like property, namely the number of barriers that $\boldsymbol{S}$ transverse in an HLM. For example, in the first kind, $\boldsymbol{S}$ may transverses one or two barriers, which is unknown. Nevertheless, in the 2nd, 3rd, and 4th kinds, the $\boldsymbol{S}$ transverses 1, 2, and 0 barriers. The topology-like property, which reveals the dynamical behavior of the spin in magnetization transversal, strongly depends on the shape of IPE and the orientation of the external field.

Figure 5 shows that the coercivity H_C, the exchange-bias field H_E, and the asymmetry of hysteresis loop can be quantitatively obtained by our approach. The value of h at the point of abrupt-flop process denotes the coercive field of descent branch H_d or ascent branch H_a. The coercivity and the EB field

can be obtained by $H_C = (H_a - H_d)/2$ and $H_E = (H_a + H_d)/2$, respectively. The length of the dotted arrows show the change of φ_S when $\boldsymbol{S}$ switches. Thus, the difference of the length of the two dotted arrows in the two branches of the HLM can describe the asymmetry of the hysteresis loop. For example, as shown in Fig. 5, the difference $\Delta\varphi_S^d - \Delta\varphi_S^a$ can describe the asymmetry of the hysteresis loop.

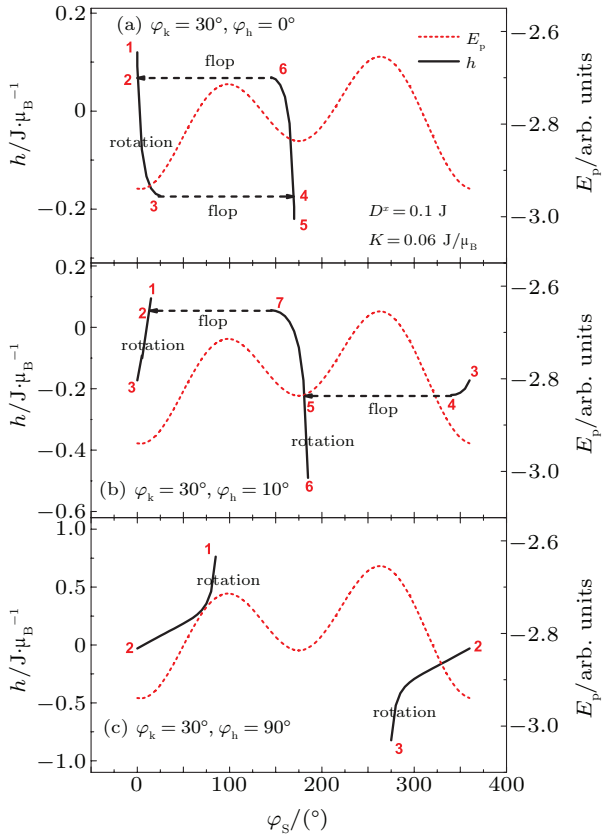


Fig. 4. (color online) Dependences of h and E_p on φ_S under different φ_h. (a) $\varphi_h = 0°$; (b) $\varphi_h = 10°$; (c) $\varphi_h = 90°$. The process of HLM is shown by solid curves and dotted arrows.

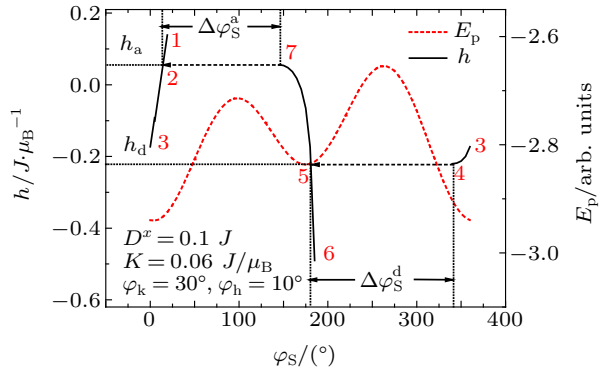


Fig. 5. (color online) Schematic for the coercive fields of the descent branch H_d and the ascent branch H_a. The $\Delta\varphi_S^d$ and $\Delta\varphi_S^a$ denote the changes of φ_S when the spin switches.

5. Summary

Base on the Stoner–Wohlfarth model, the IPE of EB systems and the stable equilibrium states of magnetization are numerically calculated. The results show that the IPE is important for understanding the intrinsic and dynamic properties of EB system. The noncollinearity between the unidirectional anisotropy and the uniaxial anisotropy can be detected by the angle between the two easy orientations of magnetization, namely, $\Delta\theta = 180°$ means collinear anisotropies, and $\Delta\theta < 180°$ means noncollinear anisotropies. In EB systems, there are four different kinds of dynamical processes underlying HLM all together, corresponding to different histories in magnetization transversal across the barriers of IPE. Interestingly, These kinds of dynamical processes can be distinguished by a topology-like property. The mechanisms of magnetization reorientation in HLM are also discussed. We show that the distribution of the stable equilibrium states is important for understanding the continuous-rotation and abrupt-flop behaviors.

References

[1] Meiklejohn W H and Bean C P 1956 *Phys. Rev.* **102** 1413
[2] Nogués J and Schuller I K 1999 *J. Magn. Magn. Mater.* **192** 203
[3] Soeya S, Hoshiya H, Arai R and Fuyama M 1997 *J. Appl. Phys.* **81** 6488
[4] Takano K, Kodama R H, Berkowitz A E, Cao W and Thomas G 1998 *J. Appl. Phys.* **83** 6888
[5] Fitzsimmons M R, Yashar P, Leighton C, Schuller I K, Nogués J, Majkrzak C F and Dura J A 2000 *Phys. Rev. Lett.* **84** 3986
[6] Hoffmann A 2004 *Phys. Rev. Lett.* **93** 097203
[7] Radu F, Westphalen A, Theis-Bröhl K and Zabel H 2006 *J. Phys.: Condens. Matter* **18** L29
[8] Cai J and Lai W 2001 *Chin. Phys. Lett.* **18** 1651
[9] Lu Z, Li T, Qiu J, Xun K, Shen H, Li Z and Shen D 1999 *Chin. Phys. Lett.* **16** 65
[10] Camarero J, Sort J, Hoffmann A, García-Martín J M, Dieny B, Miranda R and Nogués J 2005 *Phys. Rev. Lett.* **95** 057204
[11] Hu J G, Jin G J, Hu A and Ma Y Q 2004 *Eur. Phys. J. B* **40** 265
[12] Beckmann B, Usadel K D and Nowak U 2006 *Phys. Rev. B* **74** 054431
[13] McCord J, Hamann C, Schäfer R, Schultz L and Mattheis R 2008 *Phys. Rev. B* **78** 094419
[14] Jiménez E, Camarero J, Sort J, Nogués J, Mikuszeit N, García-Martín J M, Hoffmann A, Dieny B and Miranda R 2009 *Phys. Rev. B* **80** 014415
[15] Su Y, Li M, Pan J and Hu J 2012 *J. Magn. Magn. Mater.* **324** 3802
[16] Pan J, Su Y C and Hu J G 2012 *J. Magn. Magn. Mater.* **324** 1622
[17] Krivorotov I N , Leighton C, Nogués J, Schuller I K and Dahlberg E D 2002 *Phys. Rev. B* **65** 100402
[18] Mewes T, Nembach H, Fassbender J, Hillebrands B, Kim J V and Stamps R L 2003 *Phys. Rev. B* **67** 104422
[19] Tillmanns A, Oertker S, Beschoten B, Guntherodt G, Eisenmenger J and Schuller I K 2008 *Phys. Rev. B* **78** 012401
[20] McCord J, Schäfer R, Mattheis R and Barholz K U 2003 *J. Appl. Phys.* **93** 5491
[21] Yang P Y, Song C, Fan B, Zeng F and Pan F 2009 *J. Appl. Phys.* **106** 013902
[22] Saha J, Garello K, Viala B, Marty A and Vukadinovic N 2010 *Phys. Rev. B* **81** 024417
[23] Xu X Y, Tian H Y, Qian X and Hu J G 2009 *J. Appl. Phys.* **106** 093910
[24] Gao T R, Yang D Z, Zhou S M, Chantrell R, Asselin P, Du J and Wu X S 2007 *Phys. Rev. Lett.* **99** 057201
[25] Zhang X, Li L, Zhan Y, Li B and Pu F 1997 *Chin. Phys. Lett.* **14** 789
[26] Zhang X, Li L, Li B and Pu F 1998 *Chin. Phys.* **7** 518
[27] Stoner E C and Wohlfarth E P 1948 *Phil. Trans. R. Soc. A* **240** 599